Coastal Engineering 117 (2016) 157–165

Contents lists available at ScienceDirect

Coastal Engineering

journal homepage: www.elsevier.com/locate/coastaleng

Effect of overflow and seepage coupling on tsunami-induced instability of caisson breakwaters

Shinji Sassa *, Hidenori Takahashi, Yoshiyuki Morikawa, Daiki Takano

Port and Airport Research Institute, National Institute of Maritime, Port and Aviation Technology, National Research and Development Agency, 3-1-1 Nagase, Yokosuka 239-0826, Japan

ARTICLE INFO

Article history:
Received 18 March 2016
Received in revised form 29 July 2016
Accepted 8 August 2016
Available online xxxx

Keywords:
Tsunami
Overflow
Scour
Seepage
Caisson breakwater
Rubble mound

ABSTRACT

In this study, a new tsunami overflow-seepage-coupled centrifuge experimental system was developed and applied to investigate the concurrent processes, and to elucidate the mechanism, of the instability involving the scour of the mound/sandy seabed, bearing capacity failure and flow of the foundation, and the failure of caisson breakwaters, with high-resolution image analysis. A series of experiments were conducted with and without the effects of the seepage by keeping the same overflow conditions (water volume, overflow velocity, fall height and water depth), and with different mound cross-sections. All of the experiments were conducted under 50 gravities and comprised of 3 series. The first series of experiments targeted the instability of the mounds themselves by constraining the caisson movement (sliding and overturning). The second series of experiments then allowed the caisson movement and clarified how the mound scour would affect the overall stability of the caissons. The third series of experiments examined the effect of a countermeasure on the basis of the results from the two series of experiments. The experimental results first demonstrated that the coupled overflow-seepage actions promoted the development of the mound scour significantly. Notably, the scour front developed in the form of progressive slip failure at the vicinity of caissons, regardless of the mound thickness. This stems from the fact that the development of the mound scour shortened the seepage path around the shoulder area of the mound, enhancing the coupling effect of the overflow and seepage. Indeed, the scour stopped far from the caisson toe in the absence of seepage without affecting the stability of the caissons. By contrast, the scour development due to the coupled overflow-seepage approached the caisson toe and brought about bearing capacity failure of the mound, resulting in the total failure of the caisson breakwater, which otherwise remained stable without the coupling effect. The velocity vectors obtained from the high-resolution image analysis illustrated the series of such concurrent scour/bearing-capacity-failure/flow processes leading to the instability of the breakwater. The influence of placing an embankment as a countermeasure was also examined by employing different bank thickness. It is shown that the stability of the breakwaters was significantly improved with decreasing hydraulic gradient that manifested underneath the caissons due to the embankment effect. These findings will facilitate better assessment and improvement of the stability of caisson breakwaters with rubble mound foundations.

1. Introduction

The 2011 Tohoku earthquake tsunami devastated the eastern part of Japan and caused significant damage and destruction of breakwaters. The key factors contributing to the damage have been considered to be closely linked with the scour of the mound in the vicinity of breakwaters due to tsunami-induced overflow above the caissons (Arikawa et al., 2012; Arikawa and Shimosako, 2013). The seepage flow in mounds, stemming from the water level difference between offshore and onshore sides of the caissons, has also been considered to affect the stability of mounds (Takahashi et al., 2014; Sassa, 2014). However, the concrete mechanism at work in the instability of the breakwater foundation under the concurrent actions of the overflow and seepage due to a tsunami still remains unclear.

The role of tsunami-induced overflow in the performance of coastal structures has attracted recent attention in view of the stability of breakwaters, seawalls, tidewalls and dikes (Hsiao and Lin, 2010; Gulera et al., 2015; Kihara et al., 2015; Shimozono and Sato, 2016). The role of seepage in tsunami or wave-induced scour around coastal and marine structures has also been studied recently (Sumer and Fredsøe, 2002; Tonkin et al., 2003; Qi and Gao, 2014; Sumer, 2014). However, the role played by coupling of overflow and seepage in scour and the effect of this coupling on the stability of coastal structures remain poorly understood.

Against this background, the aims of this paper are, first, to clarify the processes involved in and the development of the mound scour due to tsunami-induced seepage and overflow, and secondly to investigate how the coupling actions affect the overall stability of caisson

* Corresponding author.
E-mail address: sassa@ipc.pari.go.jp (S. Sassa).

http://dx.doi.org/10.1016/j.coastaleng.2016.08.004
0378-3839/

breakwaters. For this purpose, we have developed and applied a new centrifuge experimental system which is capable of controlling the overflow and seepage due to a tsunami. A concise report of preliminary experiment using the system developed was promptly published in Sassa et al. (2014). However, this paper presents and discusses three innovations, namely, (a) by elucidating the effect of overflow and seepage coupling on the development of mound scour as obtained from the experiments with different mound cross-sections and thickness, (b) by clarifying how the overflow and seepage coupling would contribute to the collapse of caisson breakwaters, revealing the mechanism for the concurrent processes of the instability involved, and (c) by examining the influence of a countermeasure in suppressing such an effect of coupled overflow and seepage on stabilization of the caissons. The present study is based on the results of our recent study on the effect of tsunami-induced seepage on the stability of mounds in caisson breakwaters (Takahashi et al., 2014; Sassa, 2014).

2. Tsunami overflow–seepage coupled centrifuge experiment

2.1. Experimental system

It is essential to reproduce a prototype-scale stress field in the mounds that support breakwaters in order to clarify the instability of the breakwater foundations in the presence of a tsunami. A geocentrifuge makes this possible and has proved effective in studying fluid–soil interaction problems (Sassa and Sekiguchi, 1999). Indeed, the role and importance of centrifuge testing in the field of coastal and ocean engineering has recently been emphasized (Sumer and Fredsøe, 2002; Sumer, 2014). In this study, we developed and applied a new centrifuge experimental system that can simulate the combined actions of overflow and seepage due to a tsunami.

Tsunami model experiments usually model tsunami as solitary waves and thus cannot distinguish the effects of the overflow on and seepage in the mounds due to a tsunami. By contrast, in this study we constructed a system that can independently control the tsunami-induced overflow volume/rate and the water level differences causing the seepage, as shown in Fig. 1. The figure shows the system before being mounted on a centrifuge at the Port and Airport Research Institute. The mariotte water supply tank utilizes the principle of a "mariotte bottle" which enables a constant rate of flow at a constant pressure by setting the air-open interface in the tank at a prescribed location. The principle is schematically shown in Fig. 1, where the pressure at the bottom of the inlet tube is equal to atmospheric pressure, and as long as the level of water inside the tank is above the bottom of the inlet tube, the pressure at the exit hole remains constant at ρgh, realizing a constant rate of flowage. The overflow–seepage division unit controls and divides the outflow for seepage and overflow. The tank has a vertical partition that contains several drainage holes at given heights by

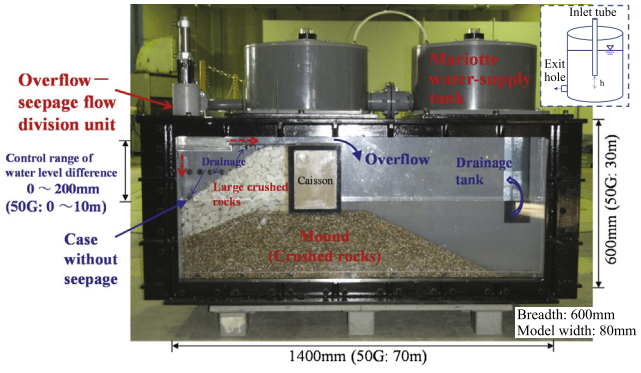

Fig. 1. Developed tsunami overflow-seepage-coupled centrifuge experimental system: The panel schematically shows the principle of the mariotte water-supply tank. Set-up for Series 1 is shown.

which to set the water level difference between the inside and outside of the caisson in the range 0–200 mm in the model, corresponding to 0–10 m under fifty gravities (50 G) on the prototype scale.

In selecting the mound material, a similitude of the seepage flow in the mound was considered together with the mechanical similarity between the model and the prototype. Specifically, the seepage flow in the mound becomes turbulent due to the high permeability of the mound (crushed rock). In this respect, a series of modeling tests were conducted, showing that one can satisfy the similitudes concerning the stress state and the turbulent seepage flow by using 1/*N*-th diameter stone as a mound material under an N-g centrifugal field in a 1/*N*-th scale model in light of a prototype in the field (Takahashi et al., 2014). In the present experiments, the mound materials had a mean grain diameter of 5 mm and the underlying sand layer had a median grain diameter of 0.18 mm. The theoretical background and the similitudes for the overflow–seepage coupled centrifuge experiment are summarized in Appendix A.

The overflow control capacity of the tank is shown in Fig. 2. Here, the overflow velocity was identified through image analysis, and the number in the parenthesis shows that on the prototype scale. This figure shows that a constant rate of overflow was maintained for a given water volume in the tank, and the duration of the constant flow rate increased with increasing water volume in the tank. Accordingly, the system realized a constant-flow-rate duration of about 10 min. on the prototype scale with an overflow speed equal to 4 m/s, which corresponds to a typical overflow state as observed during the 2011 off the Pacific coast of Tohoku Earthquake Tsunami (Arikawa et al., 2012).

2.2. Experimental design

A series of the overflow–seepage coupled centrifuge experiments using the newly developed system described above were conducted, first to investigate the stability of the mounds, and second to clarify how it would affect the overall stability of the caisson breakwaters. The centrifugal acceleration was set at 50 G. Three series of experiments were performed. In the first series (Series 1, see Fig. 1), in order to elucidate the effect of the seepage on the overflow scour, the overflow conditions, including the overflow volume, velocity, falling height from the caisson and the water depth above the mound, were all kept constant, and then the results with and without the seepage were compared. In the cases without the seepage, the water level difference between inside and outside of the caisson was set at zero, with reference to Fig. 1. In the cases with the seepage, a water level difference equal to a maximum of 8 m on the prototype scale was imposed. This maximum state means that it required some time to set-up the targeted water level difference during the experiment. The development of the mound scour was examined for two different sets of the mound width and slope, specifically 5 m and 3.5 m widths and 1:2 and 1:1.5 slopes, along with a caisson width of 10 m on the prototype scale. On the basis of these results, Series 2 examined the influence of the mound thickness on the stability of the mounds. All of the experiments in Series

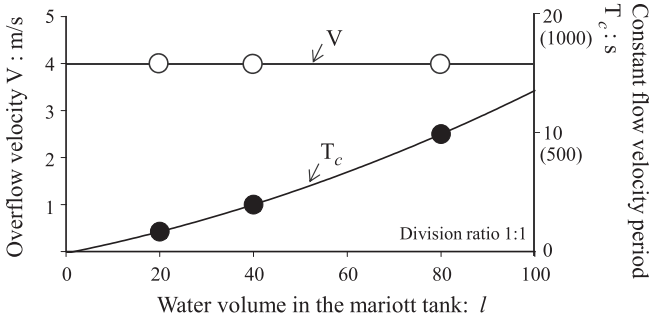

Fig. 2. Control capacity of the overflow in the tank. The values in parentheses represent those on the prototype scale. T_c represents a period where a constant flow velocity ensued.

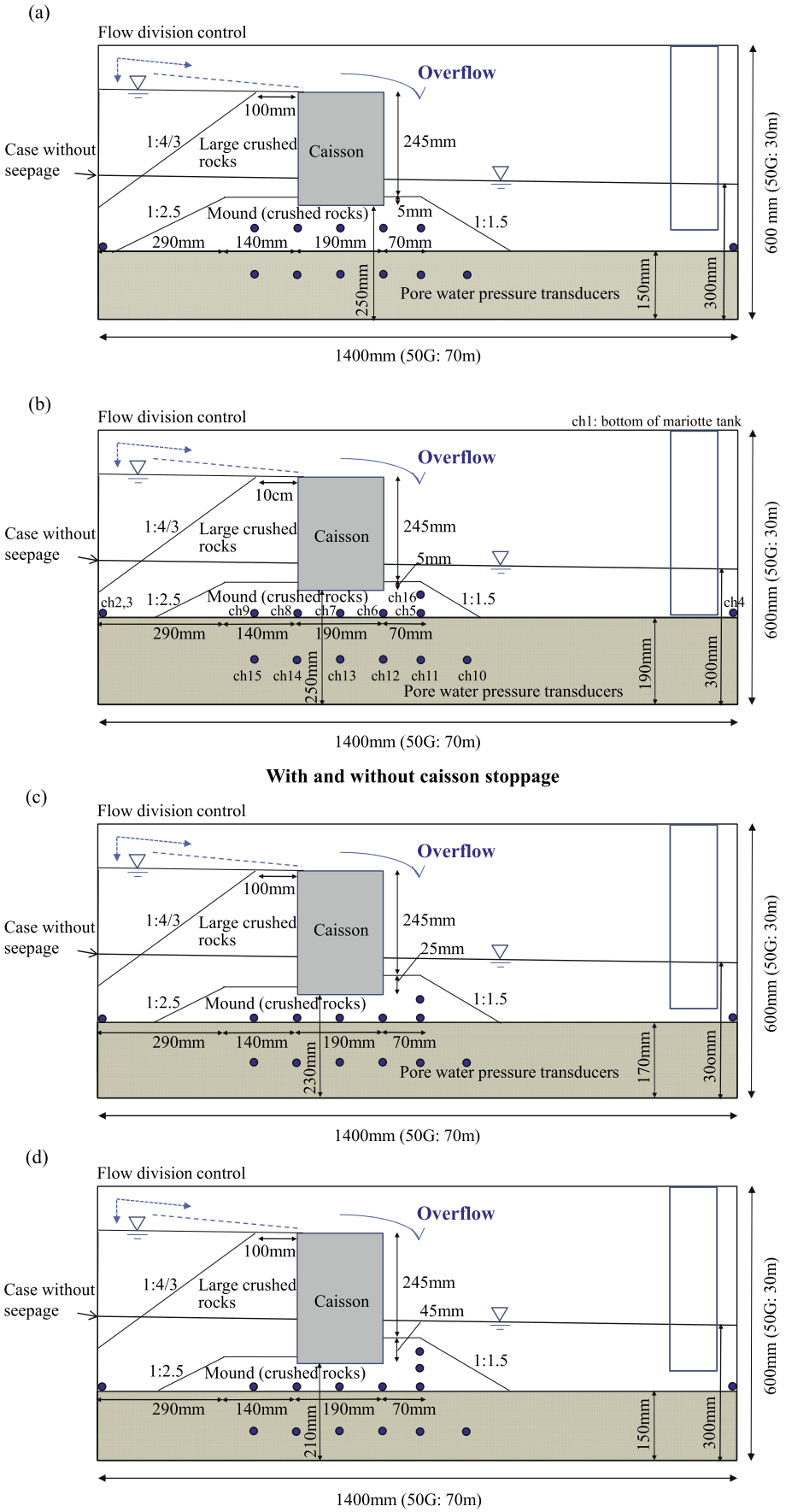

Fig. 3. Cross sections of the tsunami overflow–seepage coupled centrifuge experiment on mound scour, caisson instability and effect of embankment: (a), (b) Series 2 and (c), (d) Series 3.

1 and some of those in Series 2 were conducted by fixing the caisson movement in order to focus on the process of the instability of the mounds under the coupled actions of overflow and seepage.

With reference to Fig. 3, Series 2 allowed caisson movement by removing the caisson stoppage behind it and clarified how the mound instability would affect the instability of the caisson. Here, a smooth caisson movement was achieved by installing sponges with grease on all sides as shown in Fig. 1, thereby minimizing a friction between the caisson and the sidewalls. Series 3 examined the effect of placing an embankment as a countermeasure on the basis of the results from Series 1 and 2. In all the experiments, the dynamic processes of the mound, the foundation ground as well as the caisson under the

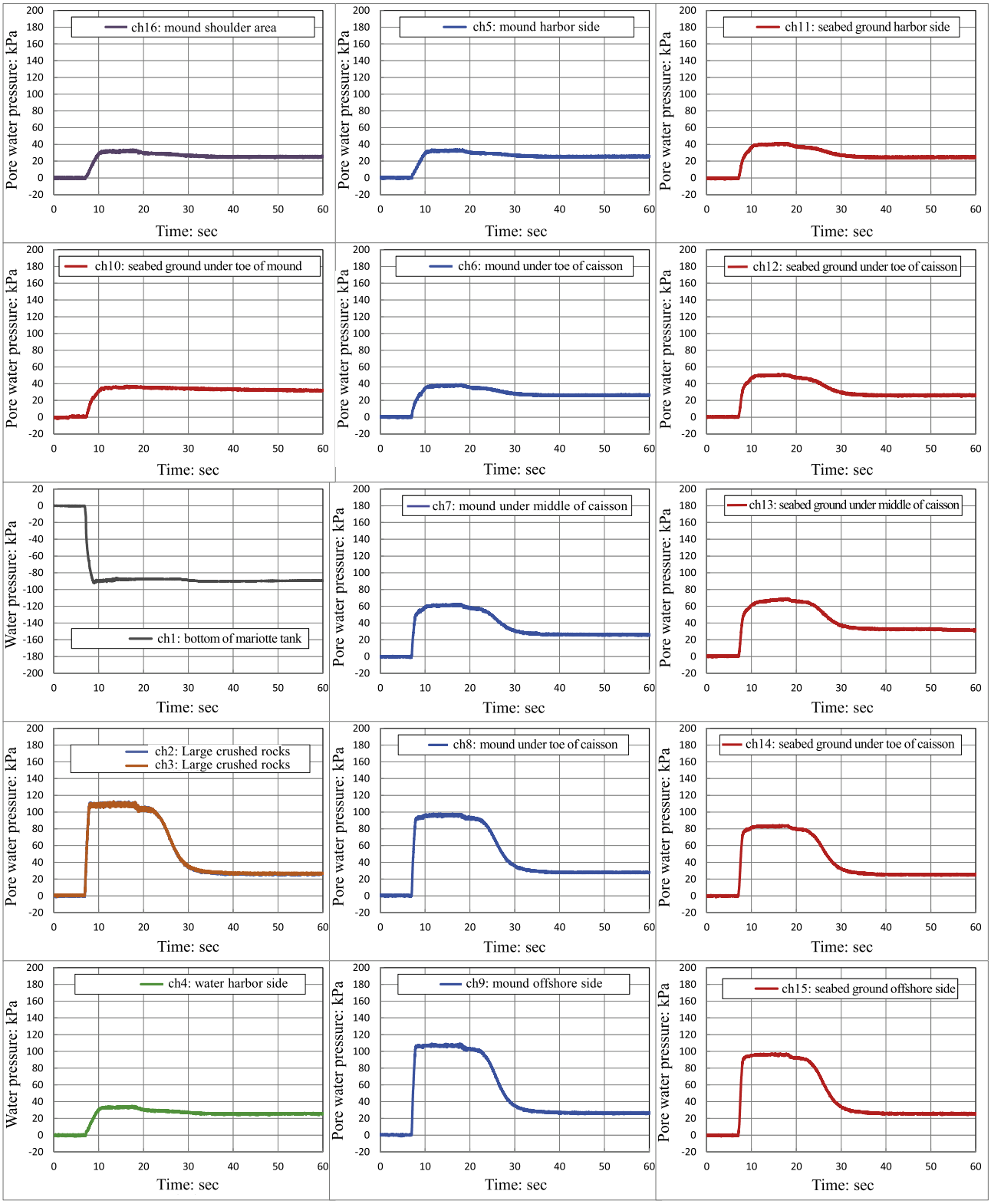

Fig. 4. Water and pore water pressures in the mound and seabed ground of the tsunami overflow-seepage coupled centrifuge experiment: This example corresponds to the cross-section in Fig. 3(b) for Series 2.

overflow with and without the seepage, were observed in the centrifuge using a CMOS camera with a maximum recording rate of 5000 frames/s. The imaging system consisted of a high-speed CMOS camera, a LED (Light Emitting Diode) lighting device mounted on the platform of the centrifuge and a control workstation connected to the high-speed camera by 1000 Base-T LAN cable via a slip ring of the centrifuge. The image obtained was analyzed by means of the digital image correlation (DIC) technique (Sutton et al., 2009; Takano et al., 2015).

The water and pore water pressures in the mound and seabed ground of the tsunami overflow-seepage coupled centrifuge experiment are shown in Fig. 4. This example corresponds to a cross-section in Fig. 3(b) from Series 2. The figure shows that a stable pressure and flow field was formed in the mound and seabed ground. It is also seen in Fig. 4 that the horizontal pressure gradients in the mound were larger than those in the seabed ground. This stems from the fact that the seepage paths were shorter in the mound that in the underlying seabed, thus yielding higher hydraulic gradients in the mound. For instance, with reference to Fig. 3(b), the difference of pore water pressures in the mounds at CH6 and CH8 which corresponded to locations under toes of caisson on harbor and offshore sides, p, reached a maximum of 60 kPa. Considering the caisson width of $D = 9.5$ m on the prototype scale, this pore water pressure difference gave rise to the hydraulic gradient of $i = p/(\gamma_w D) = 0.63$ beneath the caisson.

3. Results and discussion

3.1. Effect of overflow–seepage coupling on stability of mounds

Fig. 5 shows the results of the overflow–seepage coupled experiments for different mound shapes. Here, the initial water level coincided with the top surface of the mounds. Then, the water depth above the surface reached 2 m on the prototype scale immediately after the start of the experiment and was maintained throughout the course of the experiment. The dotted line denotes the initial geometry of the mound before undergoing scour. The results show that the development of the mound scour was closely linked with the shapes of vortexes formed below the water surface due to the overflow, and the final profiles of the scour varied significantly depending on the geometry of the mounds. Namely, for the mound with a relatively shorter width and steeper slope, the plunging effect of the overflow scoured and subsequently threw out the mound material, forming a slope far from the caisson. By contrast, for the mound with a relatively wider width and milder slope, the scoured material re-deposited in a bowl shape which was similar to the shape of the vortex formed underneath the water surface.

Fig. 6 shows the ground velocity vectors determined by the digital image correlation (DIC) technique on the development of the scour front and the flow mechanisms of the mounds observed in the vicinity

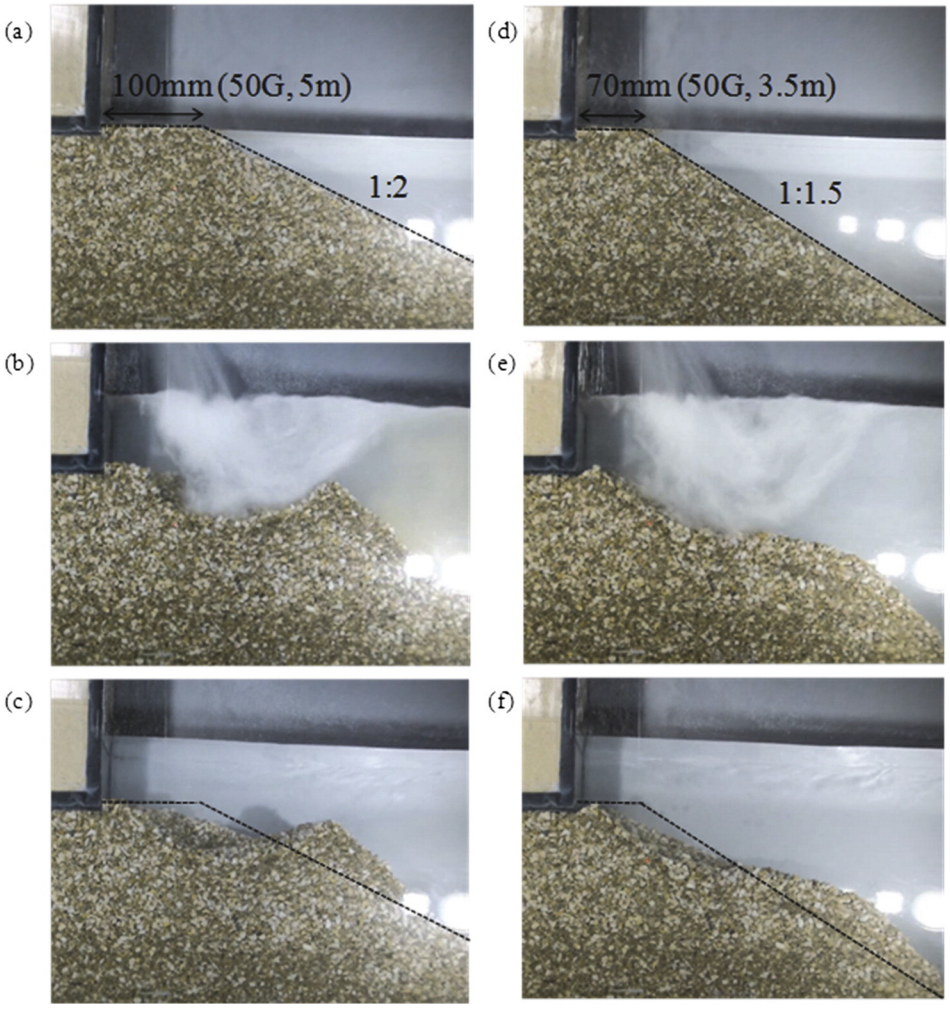

Fig. 5. Results of the overflow-seepage coupled experiment for different widths and slopes of the mounds: (a), (d) Initial (t = 0); (b), (e) Scour process (t = 5.5 s); (c), (f) Final (t = 14 s). The times represent those after commencement of overflow in the centrifuge and correspond to t = 0, 275 s, 700 s respectively on the prototype scale.

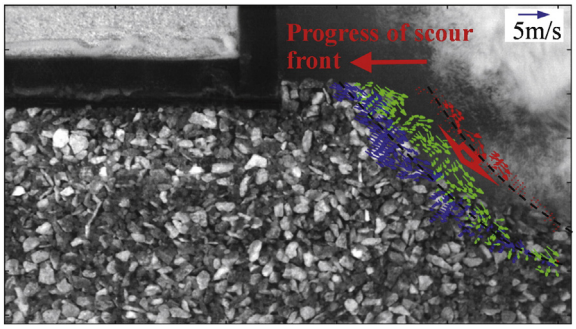

Fig. 6. Results of image analysis with high-speed CMOS camera showing the development of scour front and the flow mechanisms of the mounds.

of the caisson with seepage. This case corresponds to the condition shown in Fig. 5a, b, c, and the velocity vectors of the mound stones at three different phases are depicted in Fig. 6. The results indicate that the mound scour developed in the form of progressive slip failure, advancing toward the edge of the caisson. The associated mechanism will be described in detail later.

The seepage flow in the mound occurs in such a way that the flow direction may be essentially orthogonal to the mound slope (Takahashi et al., 2014). This means that the seepage flow reduces the frictional resistance of the mound stones against the overflow. Such coupling effects due to the combined overflow and seepage can be clarified through a comparison of the scour results with and without the seepage under the same overflow conditions, as shown in Fig. 7. One can confirm that the remaining width of the mound decreased significantly with the effects of the seepage than that without the seepage. This coupling effect became more pronounced for the mound with a relatively shorter width and steeper slope, leading to a situation where the scour front reached the toe of the caisson.

Fig. 8 shows the results of the corresponding image analysis in the vicinity of the caisson. Here, Fig. 8b shows a close-up of the velocity vectors of the mound stones, showing that the stones did not slip individually, but failed in a line along the sloping scour front. Namely, the results show that the scour developed toward the caisson in the form of progressive slip failure. As a consequence, when the scour front reached the caisson toe, the seepage path shortened, and that promoted seepage, yielding the phenomenon of significant washout (boiling). This gave rise to the formation of a cavity underneath the caisson (Fig. 8c). The wedge shaped cavity was 5 m long and 0.5 m deep on the prototype scale. The formation of such a wedge-shaped cavity is consistent with the observations using an underwater video camera conducted on site following the 2011 off the Pacific coast of Tohoku Earthquake Tsunami (NHK, 2011).

Fig. 9 shows a comparison of the maximum scour profiles, which represent the profiles of the maximum depths to which the mound materials flowed, with and without the seepage. It is seen that there is no significant difference in the maximum scour depths. This implies that the corresponding location of the maximum scour depth is far from the top of the mound, and thus the associated hydraulic gradient induced was small, so that the seepage had no appreciable effect. By contrast, the seepage path was shortest at the top surface of the mound, and therefore while a mound as wide as 1.7 m on the prototype scale remained in the absence of seepage, it completely disappeared owing to the coupling effect of the seepage and overflow in the vicinity of the caisson.

The corresponding processes of the scour development due to the coupled overflow and seepage can be more clearly seen in the form of Fig. 10, which shows the time histories of the scour front on the top surfaces of the mounds with three different thicknesses. The results demonstrate that the mound scour progressed more rapidly with seepage than without seepage, and the seepage-overflow coupling promoted the mound scour significantly. Closer examination of the processes tells us that the scour front developed rapidly and slowly cyclically, which stemmed from the fact that the mound stones failed repeatedly due to the promoted seepage on a new scour front. This confirms a distinct scour mechanism in the form of progressive slip failure due to the coupled overflow and seepage. It would be important to prevent such progressive failure from occurring in order to ensure the tsunami-resistant design of breakwater foundations.

3.2. Effect of overflow–seepage coupling on stability of caissons

The above results demonstrate the crucial role of the coupling effects of the overflow and seepage in the series of processes involving the scour development, washout, and cavity formation underneath the caisson. This knowledge should be vital in assessing and improving the stability and resilience of breakwater foundations against tsunami.

In what follows, the results from the Series 2 experiments, which clarified how the instability of the mound affected the overall stability of the caisson, are presented and discussed. With reference to Fig. 10, it is important to remark that the caisson became unstable in the shaded region where the coupling effect of the overflow and seepage on scour development manifested itself in the form of progressive slip failure of the mound. Namely, the results demonstrated that the scour development, which approached the caisson toe, due to the coupled overflow and seepage, brought about bearing capacity failure of the mound,

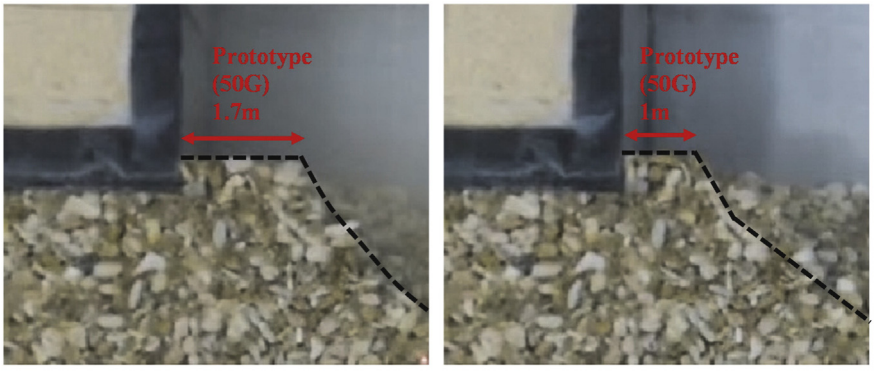

Fig. 7. Comparison of mound scour with and without tsunami-induced seepage under the same overflow conditions.

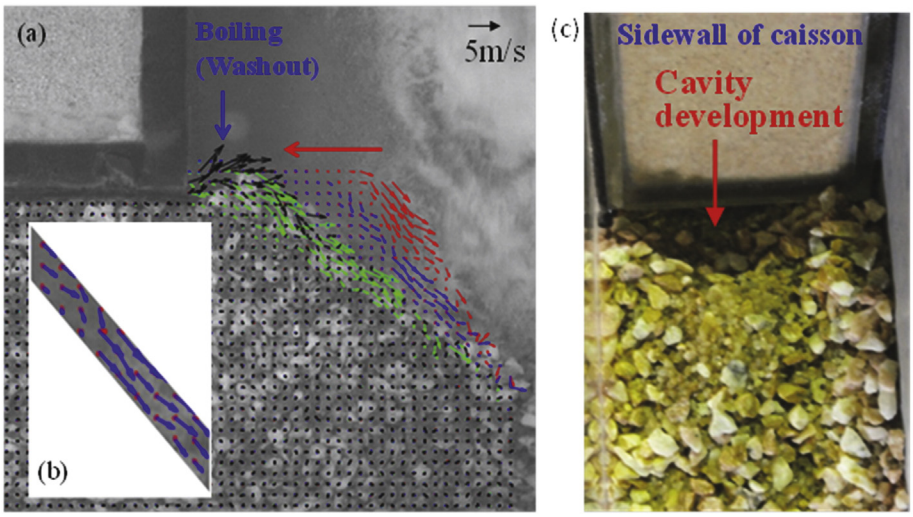

Fig. 8. Results of image analysis with high-speed CMOS camera showing the development of scour front and the flow mechanisms of the mounds: Case with washout observed.

resulting in the total failure of the caisson breakwater, which otherwise remained stable without the coupling effect. Indeed, the corresponding results of digital image correlation analyses of the observed data shown in Fig. 11 revealed the following: in the process of the scour development of the mound, as well as the seabed ground, due to the coupled overflow and seepage (Fig. 11a), the scour front approached the caisson toe, resulting in bearing capacity failure of the mound, as characterized by the upward vector of the mound stones (Fig. 11b), which gave rise to a global flow of the mound, leading to instability and collapse of the caisson (Fig. 11c).

The final configuration of the destabilized caisson due to the coupled overflow and seepage is shown in Fig. 12. The figure indicates that the caisson fell in the scour pit of the mound/seabed and subsequently the released tsunami water caused the caisson to flow away at the harbor side.

3.3. Embankment effect on stability of caissons under coupled overflow and seepage

This section addresses and clarifies the effect of placing an embankment as a countermeasure for the instability of the caisson involving the concurrent processes of the mound/seabed scour, the bearing capacity failure, and flow of the mound due to the coupled overflow and seepage, on the basis of the results from the Series 3 experiments. Here, the overflow conditions, such as the overflow velocity, fall height, and water depth, were kept constant, and only the seepage path length was varied by adopting different embankment thicknesses. The results are shown in Fig. 13, together with the results without seepage and the embankment. Here, the destabilized region of the caisson represents the region where the caisson became unstable as a consequence of the bearing capacity failure of the mound that took place because the scour development approached the caisson toe under the coupled overflow and seepage. By contrast, the stable region of the caisson represents the region where the caisson remained stable since the scour development did not approach the caisson toe and thus resulted in the absence of the bearing capacity failure of the mound. The results shown in Fig. 13 indicate that, by placing an embankment, the hydraulic gradient around the area beneath the caisson decreased, which suppressed the scour development toward the caisson toe due to the lower coupling effect of the overflow and seepage, giving rise to stabilization of the caisson. In fact, the results show that by decreasing the hydraulic gradient beneath the caisson by 0.1, that is to say, by adopting an embankment thickness of 2 m for a caisson height of 12 m, the caisson instability due to the coupled overflow and seepage can be effectively avoided under tsunami forcing conditions which would otherwise lead to caisson destabilization. These results demonstrate the utility of placing an embankment as a countermeasure for suppressing such an effect of the overflow and seepage coupling for the tsunami-resistant design of breakwaters.

4. Conclusions

In the present study, a new centrifuge experimental system that is capable of controlling the coupling actions of overflow and seepage due to a tsunami was developed to investigate tsunami-induced instability of caisson breakwaters with rubble mound foundations. The system was used with high-resolution digital image correlation analysis by means of a high-speed CMOS camera. The principal findings and conclusions obtained from three series of experiments are summarized below.

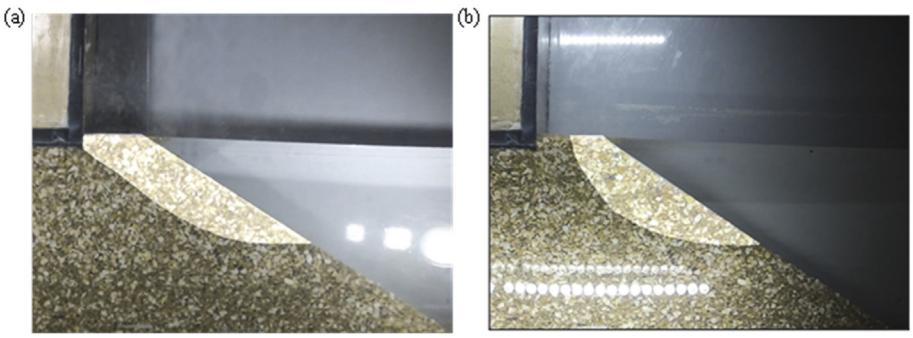

Fig. 9. Comparison of maximum scour profiles (a) with and (b) without tsunami-induced seepage.

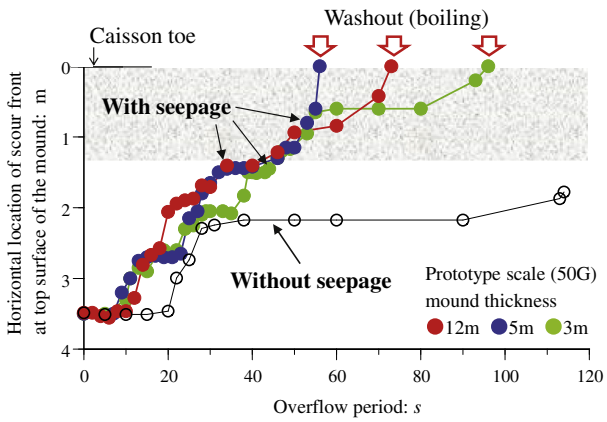

Fig. 10. Development of the mound scour due to coupled tsunami overflow and seepage, showing a distinct scour mechanism. The shaded zone indicates the region where the caisson became unstable.

Fig. 12. Final configuration of the collapsed caisson due to coupled tsunami overflow and seepage.

The results from the first and part of the second series of experiments demonstrated the way in which the scour front developed accompanying progressive slip failure of the rubble mounds, irrespective of the mound thickness. By contrast, the scour stopped far from the caisson toe in the absence of the seepage. It was found that the coupled overflow and seepage promoted the development of the mound scour considerably in the vicinity of caissons. This stemmed from the fact that the scour development shortened the seepage path, that promoted the seepage, enhancing the coupling effect of the overflow and seepage. These results gave rise to a distinct scour mechanism in the form of the progressive slip failure of the mound. The occurrence of washout and boiling as a consequence of the coupled overflow and seepage were also demonstrated, yielding a cavity formation beneath the caissons.

The combined results from the first and second series of experiments elucidated the concurrent processes of the instabilities involving the scour of the mound/seabed ground, bearing capacity failure, and flow of the mound and resulting collapse of the caisson. Notably, it was found that the scour development, approaching the toe of the caisson, due to the coupled overflow and seepage brought about the bearing capacity failure of the mound, resulting in the total failure of the caisson breakwater. This means that the overflow and seepage coupling directly affected the instability of the caisson, which otherwise remained stable without the coupling effect.

In the third series of experiments, the effect of placing an embankment as a countermeasure was examined. The embankment was shown to suppress the development of the mound scour toward the caisson toe due to the coupled overflow and seepage, in accordance with a decreasing hydraulic gradient that manifested beneath the caissons, thus preventing bearing capacity failure, resulting in stabilization of the caisson.

The observed configuration of the collapsed caisson, as well as the formation of cavities underneath the remaining caissons, are consistent with what were observed following the 2011 off the Pacific coast of Tohoku Earthquake Tsunami. Hence, these findings may facilitate better

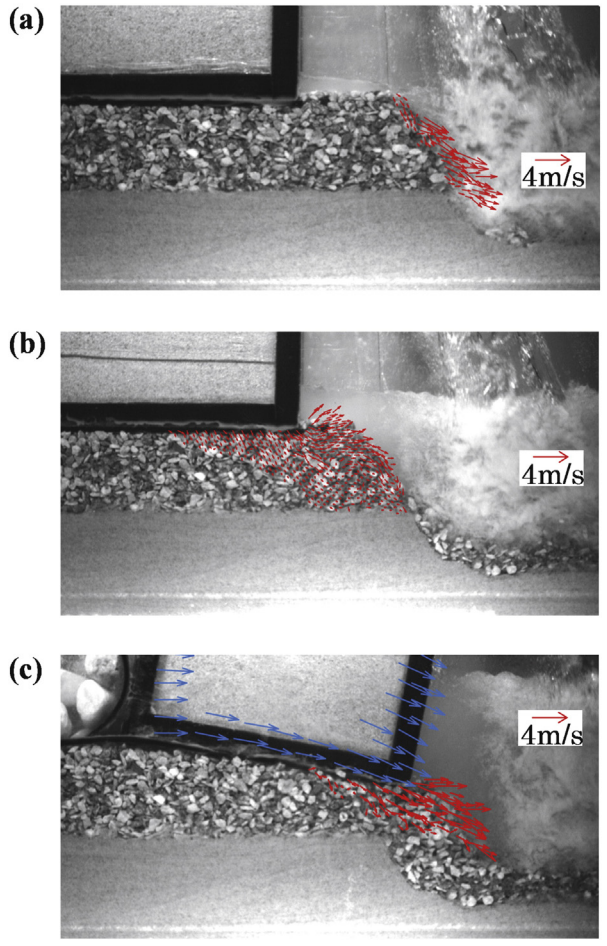

Fig. 11. Tsunami overflow and seepage coupling induced (a) scour of the mound/seabed ground, (b) bearing capacity failure, and (c) flow of the mound in the concurrent processes of the caisson instability, shown with velocity vectors. The velocity vectors correspond to those at (a) t = 15–15.25 s, (b) t = 38–44.5 s, (c) t = 55–55.25 s respectively after commencement of overflow on the prototype scale.

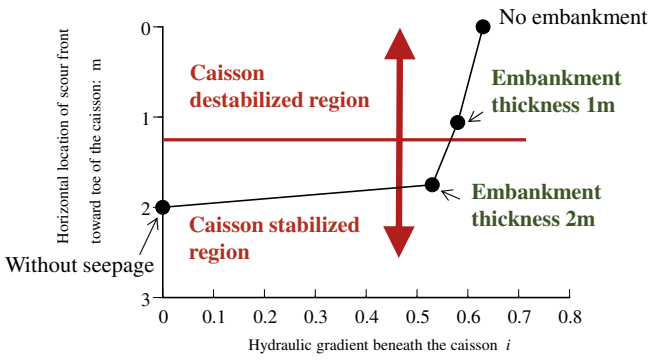

Fig. 13. Effect of embankment and the influence of hydraulic gradient on the stability of the caisson due to coupled tsunami overflow and seepage. The cases with no embankment and without seepage are shown for the purpose of comparison.

assessment, design, and improvement of the stability of caisson breakwaters with rubble mound foundations against tsunami.

Appendix A. Similitudes for the tsunami overflow–seepage coupled centrifuge experiment

The theoretical background and similitudes for the tsunami overflow–seepage coupled centrifuge experiment are described below.

Suppose that a centrifuge tsunami test with a $1/N$ scale model is performed under a constant centrifugal acceleration of Ng, where N is the scale factor, and g represents the acceleration due to the Earth's gravity. According to the Dupuit-Forchheimer approximation (Dupuit, 1863; Forchheimer, 1901; Bear, 1972; Lage, 1998; Bordier and Zimmer, 2000), the relationship between the hydraulic gradient i and mean seepage flow velocity $\bar{v}$ can be expressed as

$$i = a\bar{v} + b\bar{v}^2 \tag{1}$$

$$a = \alpha_0 \frac{\mu}{Ng}\frac{(1-n)^2}{n^3 d_{15}^2} \quad b = \beta_0 \frac{1}{Ng}\frac{1-n}{n^3 d_{15}} \tag{2}$$

The forms of Eq. (2) represent those in the widely used formulas (Carman, 1937; Ergun, 1952; Irmay, 1964; Bear, 1972; Macdonald et al., 1979; Lage, 1998, among others). Here, α_0 and β_0 are coefficients, μ is the dynamic viscosity of the pore fluid, n is the porosity of the ground, and d_{15} is the grain size passing 15% finer by weight. The hydraulic gradients in the horizontal and vertical directions can be written as

$$i_x = \frac{1}{\gamma_w}\frac{\partial \Delta u}{\partial x} = \frac{1}{\rho Ng}\frac{\partial \Delta u}{\partial x} \tag{3}$$

$$i_y = \frac{1}{\gamma_w}\frac{\partial \Delta u}{\partial y} = \frac{1}{\rho Ng}\frac{\partial \Delta u}{\partial y} \tag{4}$$

where Δu is the excess pore water pressure, γ_w is the unit weight of the fluid, and ρ is the mass density of the fluid.

In the laminar flow regime, the viscous term, i.e., the first term on the right-hand side of Eq. (1), becomes dominant. For such a Darcy flow, the associated similitude can be fulfilled by using viscous fluid whose dynamic viscosity is N-times that of water, with a hydraulic gradient and mean flow velocity equivalent to those of the corresponding prototype (Eqs. (2)–(4); Table 1). With this technique, called viscous scaling, one can satisfy the time-scaling laws for fluid wave propagation and the consolidation of the soil (Sassa and Sekiguchi, 1999). By contrast, in the turbulent flow regime, the inertia term, i.e., the second term on the right-hand side of Eq. (1), becomes dominant, for which one can satisfy the associated similitude by using the $1/N$ scale grain diameter, with a hydraulic gradient and mean flow velocity equivalent to those of the corresponding prototype (Eqs. (2)–(4); Table 1) for a given packing state. As a consequence, the time in the centrifuge model becomes a $1/N$ scale of the time in the prototype, in other words, the $1/N$ time scale is necessary to satisfy the similitude for the time, as shown in Table 1. It should be noted that the Reynolds number is not scaled here, because the Reynolds number is of the order of 10^6 with the imposed overflow velocity of 4 m/s on the centrifuge and is large enough to ignore viscous effects in the overtopping free-surface flows. The present purpose is to reproduce the fields of pore water pressure and mean seepage flow velocity and mean overflow velocity, thereby clarifying the effect of the overflow and seepage coupling on the stability of caisson breakwaters with rubble mound foundations.

Table 1
Similitudes for overflow–seepage coupled centrifuge experiment.

	Similarity ratio		
	Prototype	Present study**	Viscous scaling*
g	1	N	N
Size	1	$1/N$	$1/N$
Grain size	1	$1/N$	1
Dynamic viscosity	1	1	N
Time	1	$1/N$	$1/N$
Pressure, Stress	1	1	1
Hydraulic gradient	1	1	1
a^* or b^{**} in Eq. (1)	1	1	1
Mean seepage flow velocity	1	1	1
Mean overflow velocity	1	1	NA

NA: not applicable.
* Laminar seepage flow.
** Turbulent seepage flow.

References

Arikawa, T., Shimosako, K., 2013. Failure mechanism of breakwaters due to tsunami: a consideration to the resiliency. Proc. 6th Civil Engineering Conference in the Asian Region, Jakarta, Indonesia, pp. 1–8.

Arikawa, T., Sato, S., Shimosako, K., Tomita, T., Tatsumi, D., Ren, Y., Takahashi, K., 2012. Investigation of the failure mechanism of Kamaishi breakwaters due to tsunami - initial report focusing hydraulic characteristics. Technical Note of the Port and Airport Research Institute, 1251 (52p., in Japanese).

Bear, J., 1972. Dynamics of Fluids in Porous Media. Elsevier, New York.

Bordier, C., Zimmer, D., 2000. Drainage equations and non-Darcian modelling in coarse porous media or geosynthetic materials. J. Hydrol. 228 (3–4), 174–187.

Carman, P.C., 1937. Fluid flow through a granular bed. Trans. Inst. Chem. Eng. 15, 150–166.

Dupuit, J., 1863. Etudes Théoriques et Pratiques sur le Mouvement des Eaux. Dunod, Paris.

Ergun, S., 1952. Fluid flow through packed columns. Chem. Eng. Prog. 48 (2), 89–94.

Forchheimer, P., 1901. Wasserbewegung durch Boden. Z. Ver. Dtsch. Ing. 45 (1736–1741), 1781–1788.

Gulera, H.G., Arikawa, T., Oei, T., Yalciner, A.C., 2015. Performance of rubble mound breakwaters under tsunami attack, a case study: Haydarpasa Port, Istanbul, Turkey. Coast. Eng. 104, 43–53. http://dx.doi.org/10.1016/j.coastaleng.2015.07.007.

Hsiao, S.-C., Lin, T.-C., 2010. Tsunami-like solitary waves impinging and overtopping an impermeable seawall: experiment and RANS modeling. Coast. Eng. 57 (1), 1–18. http://dx.doi.org/10.1016/j.coastaleng.2009.08.004.

Irmay, S., 1964. Theoretical models of flow through porous media. R.I.L.E.M. Symposium on the Transfer of Water in Porous Media, Paris.

Kihara, N., Niida, Y., Takabatake, D., Kaida, H., Shibayama, A., Miyagawa, Y., 2015. Large-scale experiments on tsunami-induced pressure on a vertical tide wall. Coast. Eng. 99, 46–63. http://dx.doi.org/10.1016/j.coastaleng.2015.02.009.

Lage, J.L., 1998. The fundamental theory of flow through permeable media from Darcy to turbulence. In: Ingham, D.B., Pop, I. (Eds.), Transport Phenomena in Porous Media. Elsevier Science, Oxford, pp. 1–30.

Macdonald, I.F., El-Sayed, M.S., Mow, K., Dullien, F.A.L., 1979. Flow through porous media-the Ergun equation revisited. Ind. Eng. Chem. Fundam. 18 (3), 199–208. http://dx.doi.org/10.1021/i160071a001.

NHK: Japan Broadcasting Corporation, Tohoku Regional Bureau, Ministry of Land, Infrastructure, Transport and Tourism, Japan, 2011. Approaching the mystery of collapse of world-largest breakwaters.

Qi, W.-G., Gao, F.-P., 2014. Physical modeling of local scour development around a large-diameter monopile in combined waves and current. Coast. Eng. 83, 72–81. http://dx.doi.org/10.1016/j.coastaleng.2013.10.007.

Sassa, S., 2014. Tsunami-seabed-structure interaction from geotechnical and hydrodynamic perspectives. Geotech. Eng. J. 45 (4), 102–107 (Special Issue on Offshore and Coastal Geotechnics).

Sassa, S., Sekiguchi, H., 1999. Wave-induced liquefaction of beds of sand in a centrifuge. Géotechnique 49 (5), 621–638. http://dx.doi.org/10.1680/geot.1999.49.5.621.

Sassa, S., Takahashi, H., Morikawa, Y., Takano, D., Maruyama, K., 2014. Tsunami overflow-seepage-coupled centrifuge experiment for the mound scour. Proc. 7th International Conference on Scour and Erosion, Perth, pp. 651–656.

Shimozono, T., Sato, S., 2016. Coastal vulnerability analysis during tsunami-induced levee overflow and breaching by a high-resolution flood model. Coast. Eng. 107, 116–126. http://dx.doi.org/10.1016/j.coastaleng.2015.10.007.

Sumer, B.M., 2014. Liquefaction Around Marine Structures. Advanced Series on Ocean Engineering 39. World Scientific (472p.).

Sumer, B.M., Fredsøe, J., 2002. The mechanics of Scour in the Marine Environment. Advanced Series on Ocean Engineering 17. World Scientific (552p.).

Sutton, M.A., Orteu, J.-J., Schreier, H., 2009. Image Correlation for Shape, Motion and Deformation Measurements-Basic Concepts, Theory and Applications. Springer, New York http://dx.doi.org/10.1007/978-0-387-78747-3.

Takahashi, H., Sassa, S., Morikawa, Y., Takano, D., Maruyama, K., 2014. Stability of caisson-type breakwater foundation under tsunami-induced seepage. Soils Found. 54 (4), 789–805. http://dx.doi.org/10.1016/j.sandf.2014.07.002.

Takano, D., Lenoir, N., Otani, J., Hall, S.A., 2015. Localized deformation in a wide-grained sand under triaxial compression revealed by X-ray tomography and digital image correlation. Soils Found. 55 (4), 906–915. http://dx.doi.org/10.1016/j.sandf.2015.06.020.

Tonkin, S., Yeh, H., Kato, F., Sato, S., 2003. Tsunami scour around a cylinder. J. Fluid Mech. 496, 165–192. http://dx.doi.org/10.1017/S0022112003006402.